

Coherent optical implementation of generalized two-dimensional transforms

James R. Leger and Sing H. Lee

Department of Applied Physics & Information Science
University of California, San Diego
La Jolla, California 92093

Abstract

A coherent optical method capable of performing arbitrary two-dimensional linear transformations has recently been studied, in which transform coefficients are given by two-dimensional inner products of the input image and a set of basis functions. Since the inner product of two functions is equal to the value of their correlation when there is zero shift between the functions, it is possible to use an optical correlator to solve for the coefficients of the transform. By using random phase masks in the input and the filter planes of the correlator, we have been able to pack many coefficients close together in the output plane, and thus take better advantage of the space-bandwidth product of the optical system. Both the input random phase mask and the spatial filter are computer-generated holographic elements, created by a computer-controlled laser beam scanner. The system can be "programmed" to perform arbitrary two-dimensional linear transformations. For demonstration, the set of two-dimensional Walsh functions was chosen as a transform basis. When the resolution of the Walsh functions was limited to 128 x 128, up to 256 transform coefficients were obtained in parallel. The signal-to-noise and accuracy of the transform coefficients were compared to the theory.

Introduction

Optical processing has been shown to be a powerful technique when used to analyze two-dimensional data. Much use has been made of the lens' ability to perform two-dimensional Fourier transforms. However, there are many problems which are better solved by means of other linear transformations. The ability to tailor the transformation to a given problem is therefore highly desirable.

The intent of this paper is to show that the optical processor is not limited to Fourier analysis, but can in fact be used to perform an arbitrary two-dimensional linear transformation. In the first section, the theory of the generalized transform scheme is developed. The second section describes the experimental arrangement used to perform the transforms. Results obtained from implementing the Walsh-Hadamard transform are reported. Finally, the signal-to-noise ratio and accuracy limitations of the scheme are evaluated in the third section and compared to the experimental values.

I. Optical implementation of generalized transforms

Theory of generalized optical transform scheme¹

A coherent optical correlator is capable of performing two-dimensional correlation and convolution integrals. If a two-dimensional input has the transmittance function $g(x,y)$, and a

filter is generated which has a point spread function of $f^*(-x,-y)$, the output of the correlator is given by

$$C(-x', -y') = \iint g(x,y) f^*(x-x', y-y') dx dy \equiv f^*(x,y) \star g(x,y) \quad (1)$$

To perform a linear transformation, one wishes to express the function $g(x,y)$ as a sum of basis functions $f_{pq}(x,y)$. Assuming the set of basis functions is complete and orthonormal, $g(x,y)$ can be written as:

$$g(x,y) = \sum_{p,q} G(p,q) f_{pq}(x,y) \quad (2)$$

The transform coefficient $G(p,q)$ is given by the equation

$$G(p,q) = \iint g(x,y) f^*_{pq}(x,y) dx dy. \quad (3)$$

Comparing Eq. (3) with Eq. (1), it is seen that the central value of the correlation function is $G(p,q)$. Thus, a coherent optical correlator could be used to obtain the transform coefficient $G(p,q)$ simply by placing a transmittance function $g(x,y)$ in the input plane of the correlator, and using a spatial filter whose point spread function in inverted coordinates is the complex conjugate of the basis function $f_{pq}(x,y)$. Measuring the correlation function at its center yields $G(p,q)$. The other portions of the correlation function are of no interest, and we would like to eliminate them. This can be accomplished by multiplying $g(x,y)$ by a random phase function $\exp[i\phi_r(x,y)]$, and designing a filter which incorporates the complex conjugate of this random phase function in its point spread function. The correlation integral in Eq. (1) then becomes

$$\begin{aligned} & \iint g(x,y) \exp[i\phi_r(x,y)] f^*_{pq}(x-x', y-y') \exp[-i\phi_r(x-x', y-y')] dx dy \\ &= G(p,q) \delta(x', y'). \end{aligned} \quad (4)$$

The result that only the central value of the correlation remains is due to the fact that an ideal random mask has an autocorrelation function of a delta function $\delta(x', y')$.^{*} By using this technique, we have expressed the value of $G(p,q)$ as the amplitude of a point in correlation space.

^{*}In reality, the autocorrelation is only an approximation to a delta function, due to the finite size and resolution of the random mask. The limitation this places on the signal-to-noise and accuracy of the transform will be discussed in Section III.

Paper 1553 received Nov. 27, 1978, revised April 24, 1979. This paper is a revision of a paper presented at the SPIE seminar on Real-Time Signal Processing, Aug. 28-29, 1978, San Diego, which appears in SPIE Proceedings Vol. 154.

We can obtain many different transform coefficients simultaneously and thereby utilize the available space-bandwidth product of the optical correlator more efficiently by generating a filter which has a point spread function containing the sum of many basis functions. To separate the transform components in the correlation space, the conjugate of each basis function is multiplied by the conjugate random phase mask, and a sum is formed from shifted versions of these products. The point spread function of the filter becomes

$$h^*(-x, -y) = \sum_{p,q} f^*_{pq}(x-p\Delta, y-q\Delta) \exp[-i\phi_r(x-p\Delta, y-q\Delta)] \quad (5)$$

where $f_{pq}(x, y)$ are the basis functions,

$\phi_r(x, y)$ is a random function,

Δ is a shift constant.

The correlation integral of Eq. (1) becomes

$$\begin{aligned} & \iint g(x, y) \exp[i\phi_r(x, y)] \sum_{p,q} f^*_{pq}(x-x'-p\Delta, y-y'-q\Delta) \\ & \quad \exp[-i\phi_r(x-x'-p\Delta, y-y'-q\Delta)] dx dy \\ &= \sum_{p,q} G(p, q) \delta(x' + p\Delta, y' + q\Delta). \end{aligned} \quad (6)$$

The optical implementation of this operation is shown in Figure 1.

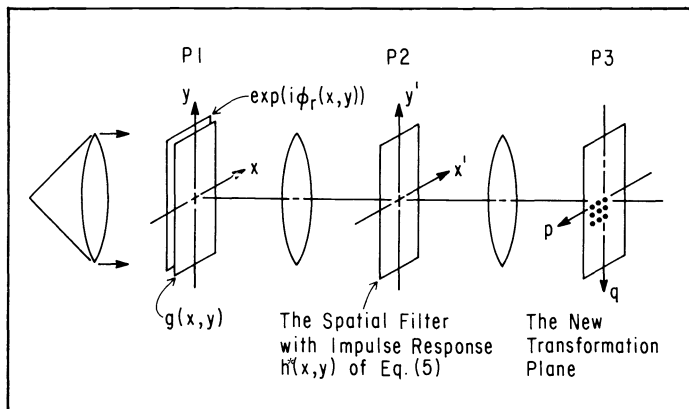


Figure 1. One possible optical configuration for performing generalized transformations. A random phase mask $\exp[i\phi_r(x, y)]$ is placed in contact with the input function $g(x, y)$. The transform coefficients are displayed simultaneously in a 2-dimensional array at plane P3.

It consists of inserting a random phase filter in the input plane P1 and using a spatial filter in plane P2 whose point spread function is given by Eq. (5). Plane P3 contains the transform coefficients spaced by an amount proportional to Δ .

II. An experimental system for performing generalized transformations

A. Optical correlator

In order to implement the optical setup shown in Figure 1, one must fabricate two optical elements. The first one is the random phase mask in plane P1, whose transmittance is a pure phase function described by $\exp[i\phi_r(x, y)]$. The second element is the spatial filter, whose transmittance must be equal to the Fourier transform of $h^*(-x, -y)$ given in Eq. (5). This transmittance is in general a complex function, implying that both the amplitude and phase of the light must be modulated. The first element could be made by

bleaching a piece of film which was exposed to a pattern of random intensity values. But, in order to match the random phase mask transmittance of the first element in P1 to the complex conjugate of the random phase mask encoded in the filter at plane P2, it is simpler to generate the first random phase mask as well as the filter by computer as computer-generated holograms. This way, any difference in producing the random phase functions is minimized, yielding a better approximation to the delta function when they are correlated.

The experimental arrangement which was actually used is diagrammed in Figure 2. A plane wave illuminates plane P0

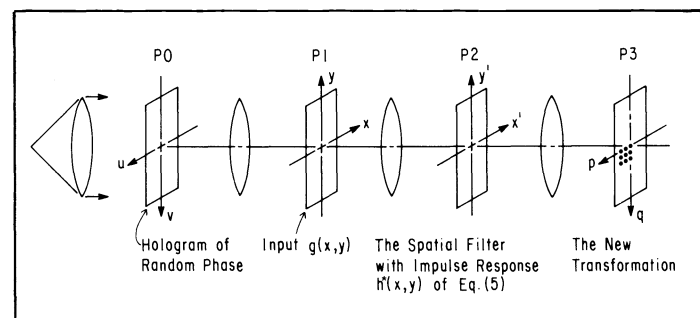


Figure 2. Experimental setup to perform generalized transforms. A hologram at P0 reconstructs the phase function $\exp[i\phi_r(x, y)]$ in plane P1.

which contains a computer-generated hologram whose point spread function is $\exp[i\phi_r(x, y)]$. This function reconstructs at plane P1 and illuminates the input. The amplitude of the light just past P1 is the product of the input function $g(x, y)$ and the random phase function $\exp[i\phi_r(x, y)]$. This product is correlated with the point spread function of the spatial filter in P2, and the resulting inner products appear in plane P3.

B. Hologram synthesis

The two optical elements in planes P0 and P2 are computer-generated holograms.^{2,3} Each pixel of the hologram is comprised of three dots of equal spacing but different transmittance. Even when different types of transforms are desired, the random phase hologram in plane P0 can stay the same and so needs to be created only once. The filter hologram in plane P2, however, will have to be changed. To control the type of transform, one would like to be able to create this filter automatically by a computer-controlled laser beam scanner.

The laser beam scanning system we constructed consists of an acousto-optic modulator combined with a pair of galvanometer-driven mirrors, all interfaced to a microcomputer (see Figure 3).

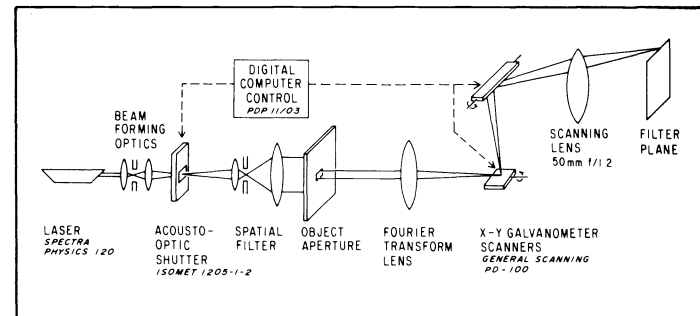


Figure 3. The laser beam scanning system.

The galvanometer mirrors are mounted such that one controls the X position of the beam, and the other controls the Y position. The modulator simply acts as a very fast shutter. With this system, a grid of 1500 x 1500 cells of arbitrary transmittance can be placed



Figure 4. Photomicrograph of the center of a computer-generated holographic filter. This hologram consists of 786,432 rectangular apertures of varying transmittance. The size of the hologram is 1.4 cm x 1.4 cm. Each aperture is approximately 10 x 20 microns in size.

in a 2 cm² area of film (see Figure 4). An interrupt-driven parallel interface allows the microcomputer to run both mirrors and the modulator.

The system represents a great improvement over other methods of generating computer holograms such as with a CAL-COMP plotter or a CRT because the laser scanner system makes holograms of the proper size, whereas other holograms must be photographically reduced. The CAL-COMP plotter can generate approximately the same number of apertures as the laser scanner system, but it can provide only binary transmittances and takes a long time to draw one hologram. The CRT is fast, but lacks the spatial uniformity of grey scale and resolution, along with having distortions in the corners.

C. Experimental results from the Walsh-Hadamard transform

One linear transformation which is of practical interest is the Walsh-Hadamard transform. The basis functions are defined by successive Kronecker products of the 2 x 2 Hadamard matrix

$$\begin{bmatrix} 1 & 1 \\ 1 & -1 \end{bmatrix},$$

and in their Walsh-ordered form, they resemble square waves of varying periodicity.

Using the computer-controlled scanning system, both the random phase and filter holograms were generated. Each hologram consisted of 128 x 128 resolution cells and was replicated four times in both the X and Y directions.* The point spread function of the random phase hologram, $\exp[i\phi_r(x,y)]$, was designed to appear in the +1 diffraction order, where $\phi_r(x,y)$ is a random function uniformly distributed between 0 and 2π . The complex conjugate of the function appeared in the -1 diffraction order. Similarly, the point spread function of the spatial filter hologram was:

$$h(x,y) = \sum_{p=1}^L \sum_{q=1}^L \text{WAL}_{pq}(x-p\Delta, y-q\Delta) \exp(i\phi_r(x-p\Delta, y-q\Delta)) \quad (7)$$

*The replication makes the correlation points sharper and brighter, without introducing the computational difficulties (long computational time and large computer memory) associated with high resolution computer-generated holograms.

in the +1 diffraction order, and $h^*(-x,-y)$ in the -1 diffraction order. $\text{WAL}_{pq}(x,y)$ is the (p,q)th Walsh function, and Δ is proportional to the spacing of the transform coefficients in the correlation plane.

By masking off all but the +1 order reconstruction of the random phase hologram in plane P1 of Figure 2, and all but the -1 order reconstruction of the spatial filter hologram in plane P3, $N = L^2$ transform dots were obtained simultaneously in plane P3. The number of transform components (N) was varied from 16 to 256. The amplitude of each of these dots is proportional to the corresponding Walsh component of the input.

Several geometrical figures were used as input objects. Figure 5 shows three of these objects, and the resulting output from the optical correlator. This can be compared with the square of the transform performed by an electronic computer and displayed on a TV screen. The comparisons are in good general agreement. The SNR and the accuracy of the transform coefficients are assessed in the following section.

III. Signal-to-noise ratio and accuracy considerations

In the analysis given in Section I, it was assumed that the autocorrelation of a random phase mask was a delta function. In practice, however, when one is constrained to use masks which are finite in both size and resolution, the autocorrelation function will have some energy in the sidelobes. The extraneous light in the sidelobes gives rise to noise which sets a fundamental limit on the performance of the system. The equations governing the noise power and the intensity signal-to-noise ratio (SNR) are derived below in a manner similar to that used to analyze coded multiple exposure holograms.⁴ The effect of this noise on the accuracy of the transform coefficients is then considered.

In order to reduce the complexity of the analysis, two simplifications are made. First, the input function as well as the basis functions are assumed to have unity amplitude. Secondly, one-dimensional notation is used. Extension to two dimensions is straightforward.

If the one-dimensional space-bandwidth product of both computer-generated holograms in planes P0 and P2 of Figure 2 is M, then each is able to reconstruct M points. In particular, the hologram at P0 creates M points of unity magnitude and random phase in its first order reconstruction at the input plane P1:

$$U(x) = \sum_{m=0}^{M-1} \delta(x-md) \exp[+i\phi_r(x)] \quad (8)$$

where d is the spacing between points in plane P1, and $\phi_r(x)$ is a uniformly distributed random phase function.

Assuming that plane P1 is filtered to allow only the first order to pass and that the input function in P1 is unity, the light incident on plane P2 will be the Fourier transform of Eq. (8):

$$\begin{aligned} U(x') &= \int \sum_{m=0}^{M-1} \delta(x-md) \exp[+i\phi_r(x)] \exp\left[-i2\pi\left(\frac{x'}{\lambda f}\right)x\right] dx \\ &= \sum_{m=0}^{M-1} \exp[+i\phi_r(md)] \exp\left[-i2\pi\left(\frac{mdx'}{\lambda f}\right)\right]. \end{aligned} \quad (9)$$

Thus we see that the amplitude at plane P2 formed from the M points of random phase at P1 consists of M plane waves with propagation angles $\theta = \cos^{-1}(md/f)$ and phases $\phi_r(md)$.

The transmittance of the spatial filter at plane P2 was computed by performing a digital Fourier transform on the impulse

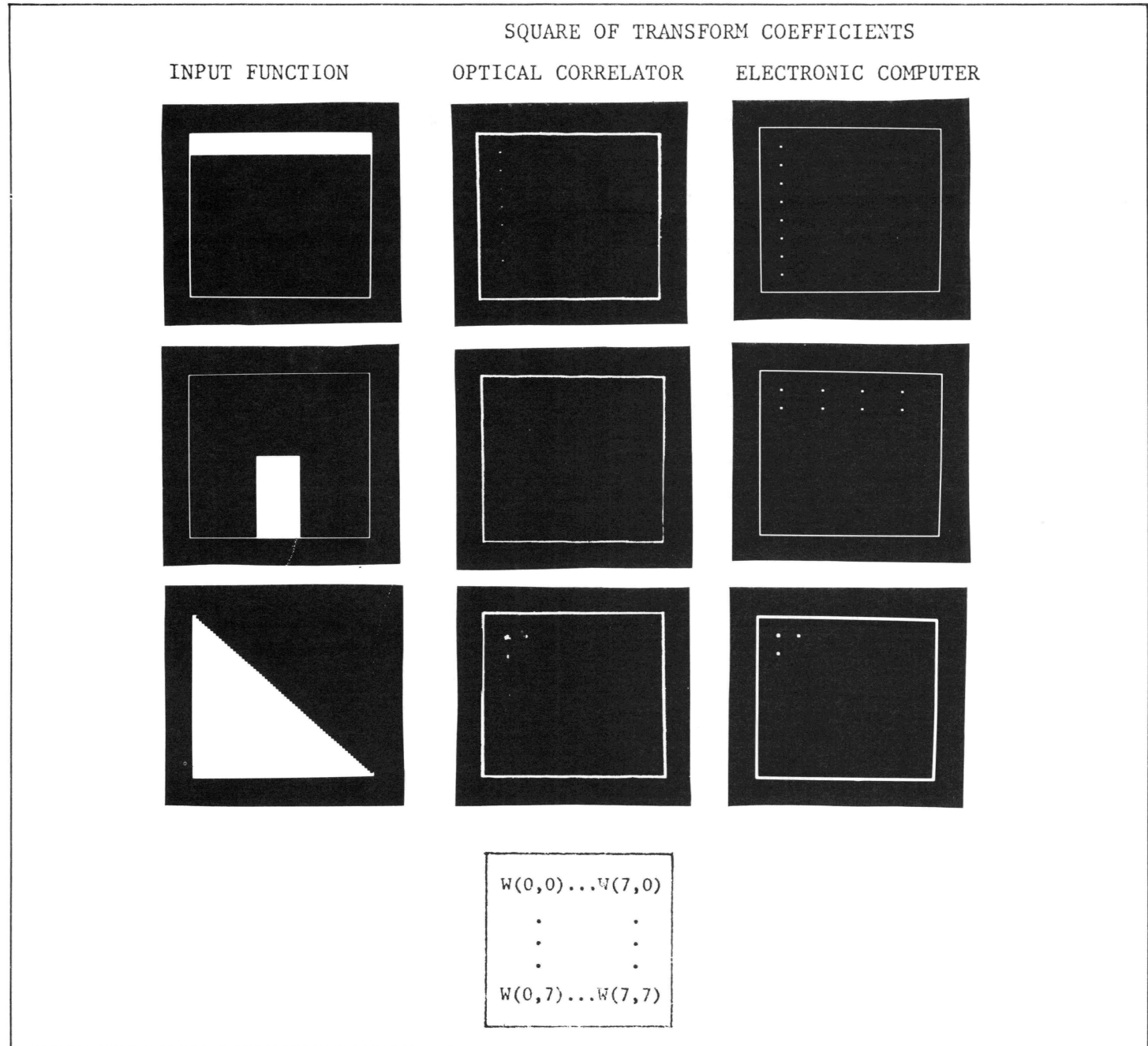


Figure 5. The output of the optical correlator (middle column) is compared to the solution obtained by an electronic computer (right column) for 3 input objects. The intensity of the spots is proportional to the square of the transform coefficients in both cases. The placement of coefficients is diagrammed in the bottom square.

response given in Eq. (5). Since one of the assumptions of this analysis is that the basis functions $f_{pq}(x,y)$ are unity, the impulse response of Eq. (5) will be simplified to

$$h^*(-x) = \sum_{k=0}^{N-1} \exp[-i\phi_r(x-k\Delta)] \quad (10)$$

where N is the number of superimposed functions corresponding to the number of simultaneous transform coefficients.

Sampling Eq. (10) with a spacing of d between sample points, we have

$$h^*(-x) = \sum_{k=0}^{N-1} \sum_{m=0}^{M-1} \delta(x-md) \exp[-i\phi_r(x-k\Delta)]$$

or

$$h^*(x) = \sum_{k=0}^{N-1} \sum_{m=0}^{M-1} \delta(x + md) \exp[-i\phi_r(-x-k\Delta)] \quad (11)$$

Digitally Fourier transforming Eq. (11) and scaling it by a factor of $1/\lambda f$, we obtain the transmittance function of the spatial filter at plane P2:

$$\begin{aligned}
 t(x') &= \int \sum_{k=0}^{N-1} \sum_{m=0}^{M-1} \delta(x + md) \exp[-i\phi_r(-x - k\Delta)] \exp[-i2\pi(\frac{x'}{\lambda f})] dx \\
 &= \sum_{k=0}^{N-1} \sum_{m=0}^{M-1} \exp[-i\phi_r(md - k\Delta)] \exp[i2\pi(\frac{mdx'}{\lambda f})]. \quad (12)
 \end{aligned}$$

The light field leaving the filter can be described as the product of Eq. (9) and Eq. (12):

$$\begin{aligned}
 U'(x') &= U(x') t(x') \\
 &= \left\{ \sum_{m=0}^{M-1} \exp[i\phi_r(md)] \exp\left[-i2\pi(\frac{mdx'}{\lambda f})\right] \right\} \\
 &\quad \left\{ \sum_{k=0}^{N-1} \sum_{m'=0}^{M-1} \exp[-i\phi_r(m'd - k\Delta)] \exp\left[+i2\pi(\frac{m'dx'}{\lambda f})\right] \right\} \\
 &= \left\{ \sum_{k=0}^{N-1} \sum_{m=0}^{M-1} \sum_{m'=0}^{M-1} \exp\left[-i2\pi\frac{(m-m')d}{\lambda f} x'\right] \right. \\
 &\quad \left. \exp[i\phi_r(md) - i\phi_r(m'd - k\Delta)] \right\} \quad (13)
 \end{aligned}$$

Equation (13) can be interpreted as consisting of NM^2 plane waves propagating at angles $\theta = \cos^{-1}[(m-m')d/f]$ and of phases $[\phi_r(md) - \phi_r(m'd - k\Delta)]$.

The third lens in Figure 2, of focal length f , performs a final Fourier transformation on Eq. (13).

$$\begin{aligned}
 U(p) &= \int \sum_{k=0}^{N-1} \sum_{m=0}^{M-1} \sum_{m'=0}^{M-1} \exp\left[-i2\pi\frac{(m-m')d}{\lambda f} x'\right] \\
 &\quad \exp[i\phi_r(md) - i\phi_r(m'd - k\Delta)] \exp\left[-\frac{i2\pi x'}{\lambda f} p\right] dx' \\
 &= \sum_{k=0}^{N-1} \sum_{m=0}^{M-1} \sum_{m'=0}^{M-1} \delta(p - (m-m')d) \exp[i\phi_r(md) - i\phi_r(m'd - k\Delta)] \quad (14)
 \end{aligned}$$

Since we are only interested in the light amplitude of a specific point, for example at the origin, then $U(p=0)$ can be evaluated by applying the condition $m = m'$ in Eq. (14):

$$U(p=0) = \sum_{k=0}^{N-1} \sum_{m=0}^{M-1} \delta(p) \exp[i\phi_r(md) - i\phi_r(md - k\Delta)] \quad (15)$$

Equation (15) can be broken up into two terms by separating the

components of identical phase ($k=0$) from the random phase components ($k \neq 0$):

$$U_1(p=0) = \sum_{m=m'=0}^{M-1} \delta(p) = M \delta(p) \quad (16)$$

$$U_2(p=0) = \sum_{k=1}^{N-1} \sum_{m=m'=0}^{M-1} \delta(p) \exp[i\phi_r(md) - i\phi_r(m'd - k\Delta)] \quad (17)$$

The signal amplitude for unity amplitude input function and basis functions is given by Eq. (16) and consists of M delta functions of identical phase. Equation (17) indicates that the total noise amplitude at this same point consists of $(N-1)M$ delta functions of unrelated phase.

The intensity of the signal (I_s) is simply given by

$$I_s = U_1(0) U_1^*(0) = M^2. \quad (18)$$

The noise term on the other hand can only be described statistically due to the random phases associated with each of the delta functions. Since the magnitude of each of these delta functions is unity, random walk statistics apply. Therefore, the expected value of the noise intensity is the sum of intensities of the delta functions in Eq. (17):

$$\bar{I}_N = (N-1)M. \quad (19)$$

An intensity signal-to-noise ratio can now be defined as the ratio of signal intensity to mean noise intensity:

$$\text{SNR} = \frac{I_s}{\bar{I}_N} = \frac{M^2}{(N-1)M} = \frac{M}{(N-1)} \quad (20)$$

where M and N are respectively defined earlier as the space bandwidth product of the random phase holograms and the number of superimposed holograms (or equivalently the number of simultaneous transforms). This result is as expected, since the autocorrelation of a random phase mask with a very high space-bandwidth product (M) is close to an ideal delta function and so increases the SNR. On the other hand, as the number of simultaneous transforms (N) is increased, each of the random phase functions associated with a basis function contributes to the overall noise and lowers the SNR.

To verify this SNR analysis, an experiment was performed with a constant input function. The intensity of the $\text{WAL}(0,0)$ transform coefficient* was compared to the background noise intensity.

A scanning fiber optic probe and photomultiplier tube were used to make these measurements. The values of the SNR presented in Table 1 were all obtained using filters with 128×128 resolution cells (i.e. $M = 16,384$), but various numbers of simultaneous transforms (N).

The fact that the experimental SNR is smaller than theoretical predictions can be attributed to the presence of other sources of noise which include the inherent errors in computer-generated holograms,^{5,6} the positional accuracy of the laser scanning system, and the nonlinearities and finite dynamic range of the filter recording material.

The accuracy of the magnitude and phase of a measured transform coefficient is fundamentally limited by the noise present

*The noise at this point corrupts any measurement of the signal intensity. However, if the SNR is large, it can be shown that the expected value of the intensity is simply the signal intensity.

Table 1. SNR of WAL(0,0) transform coefficient

Number of Simultaneous Transforms (N)	Experimental Intensity SNR (db)	Theoretical Intensity SNR (db) = $10 \log_{10} \frac{M}{N-1}$
16	21	30
64	15	24
256	13	18

at the signal point and therefore can be related to the intensity SNR. Because coherent light is being used, the signal and the noise add in amplitude. The mean and standard deviation of the resultant magnitude r and phase θ can be calculated in general as shown in Ref. 7 and 8. However, if the SNR $\gg 1$, the noise component does not affect the mean magnitude and therefore the mean magnitude is simply given by $\bar{r} = \sqrt{\bar{I}_s}$. Similarly, the variance of the magnitude is not affected by the signal, and is therefore given by $\sigma_r^2 = (\bar{I}_n/2)$. The variance of the phase is given by $\sigma_\theta^2 = (I_N/2\bar{I}_s)$. Thus, the accuracy of a transform coefficient can be stated as:

$$\begin{aligned} \frac{\sigma_r}{\bar{r}} &= \frac{\sqrt{\frac{\bar{I}_N}{2}}}{\sqrt{\bar{I}_s}} = \sqrt{\frac{(N-1)}{2M}} = \frac{1}{\sqrt{2(\text{SNR})}} \\ \sigma_\theta &= \sqrt{\frac{\bar{I}_N}{2\bar{I}_s}} = \sqrt{\frac{(N-1)}{2M}} = \frac{1}{\sqrt{2(\text{SNR})}} \end{aligned} \quad (21)$$

It can be seen that the accuracy of the magnitude and phase is proportional to the inverse square root of the intensity SNR. This result is expected, since the signal and noise terms interact in amplitude rather than intensity, resulting in a ratio of square roots of intensities.⁹

Equation (21) allows one to relate the accuracy of the magnitude and phase of a transform coefficient to the intensity SNR. The values σ_r/\bar{r} and σ_θ are presented in Table 2, based on

Table 2. Magnitude and phase accuracy of the WAL(0,0) transform coefficient

Number of Simultaneous Transforms (N)	Experimental		Theoretical	
	σ_r/\bar{r}	σ_θ	σ_r/\bar{r}	σ_θ
16	6%	4°	2%	1.3°
64	12%	7°	4%	2.6°
256	16%	9°	9%	5°

the theoretical calculations and experimental measurements of the SNR given in Table 1. The values are given for various number of simultaneous transform coefficients, using a filter with 128 x 128 resolution cells. The accuracy as well as the SNR can be improved by using random phase masks and spatial filters which have larger space-bandwidth products.

Conclusion

An optical system has been investigated which makes effective use of the space-bandwidth product of a coherent optical correlator for implementing generalized two-dimensional transforms. The intensity signal-to-noise ratio of the transformation, as well as the accuracy of the coefficients, has been shown to be a function of the space-bandwidth product of the random phase filters and the number of transform coefficients to be computed. Higher SNR, more transform coefficients, and greater accuracy are achievable if one employs filters with larger space-bandwidth products. For example, the theoretical accuracy limit of a filter with a space-bandwidth product of 512 x 512, designed to produce 64 simultaneous transform coefficients is 1% in magnitude and 0.6° in phase. Its theoretical SNR is 36 db. The resolution of the input function and the basis functions is 512 x 512 points. Since the spatial filter needs changing only once when a different type of transform is desired, large space-bandwidth filters could be created and used for processing large amounts of data.

The optical system appears to be ideally suited for applications where high resolution is required in the input plane, and only a modest number of transform coefficients are needed. Such applications are frequently found in pattern recognition problems and include feature selection as well as linear classification from feature space to decision space.

Acknowledgments

We acknowledge the support of this work by the National Science Foundation and the Air Force Office of Scientific Research.

References

- Lee, S. H., "Mathematical operations by optical processing," *Optical Engineering* 13, 196-207 (1974).
- Lee, W. H., "Sampled Fourier transform hologram generated by computer," *Appl. Opt.* 9, 639-643 (1970).
- Burckhardt, C. B., "A simplification of Lee's method of generating holograms by computer," *Appl. Opt.* 9, 1949 (1970).
- La Macchia, J. T., and D. L. White, "Coded multiple exposure holograms," *Appl. Opt.* 7, 91-94 (1968).
- Allebach, J. P., N. C. Gallagher, and B. Liu, "Aliasing errors in digital holography," *Appl. Opt.* 15, 2183-2188 (1976).
- Gabel, R. A., "Reconstruction errors in computer generated binary holograms: a comparative study," *Appl. Opt.* 14, 2252-2255 (1975).
- Schwartz, M., *Information Transmission, Modulation, and Noise*, McGraw-Hill, New York, pp. 392-422, 1959.
- Papoulis, A., *Probability, Random Variables, and Stochastic Processes*, McGraw-Hill, New York, pp. 498-501, 1965.
- Collier, R. J., C. B. Burckhardt, and L. H. Lin, *Optical Holography*, Academic Press, Inc., New York, pp. 355-357, 1971. ◇